European Journal of Applied Sciences – Vol. 13, No. 04
Publication Date: August 15, 2025
DOI:10.14738/aivp.1304.19227.
Duc, D. M., & Quang, P. (2025). Numerical Simulation of the Solidification Process of Aluminum Alloys Using ABAQUS Finite Element Software. *European Journal of Applied Sciences*, Vol - 13(04). 223-230.

Numerical Simulation of the Solidification Process of Aluminum Alloys Using ABAQUS Finite Element Software

Do Minh Duc
School of Materials Science and Engineering,
Hanoi University of Science and Technology (HUST), Hanoi, Viet Nam

Pham Quang*
School of Materials Science and Engineering,
Hanoi University of Science and Technology (HUST), Hanoi, Viet Nam

ABSTRACT
This study presents a detailed numerical simulation of the solidification process of aluminum alloys using ABAQUS finite element software. A 2D axisymmetric thermal model was developed to capture transient temperature fields, phase transitions (solid, semi-solid, and liquid), and solidification-front propagation in a stepped mold geometry. Results show how variations in mold thickness affect thermal gradients and consequently influence microstructure and mechanical properties. The simulation highlights the critical role of cooling rates in different mold zones and offers predictive insights into potential casting defects such as porosity and shrinkage. The methodology offers a cost-effective and robust approach for optimizing mold design and thermal control in aluminum casting.

Keywords: Solidification, Aluminum Alloys, ABAQUS Simulation, Thermal Analysis, Phase Change, Casting Defects, Mushy Zone, Heat Transfer.

INTRODUCTION
Solidification is a pivotal stage in metal casting that critically determines the final microstructure, defect formation, and mechanical performance of cast components. Accurate control and prediction of thermal gradients and solid–liquid interface behavior during this stage can significantly reduce casting defects such as porosity, hot tearing, and inhomogeneous grain formation [1,2].

Aluminum alloys, particularly casting grades like A356, AlSi10Mg, and AlSi7Cu, are widely used in automotive and aerospace applications due to their excellent strength-to-weight ratios, good corrosion resistance, and high castability [3]. However, these alloys exhibit complex solidification behavior influenced by mold geometry, boundary conditions, and alloy composition. Non-uniform cooling can lead to microstructural heterogeneities and mechanical weakness [4].

Recent advances in numerical simulation have enabled better understanding and control of heat transfer and phase change during solidification [5-10]. While specialized casting simulation software such as ProCAST or MAGMASoft exists,… [11-13], general-purpose tools

* Corresponding Author: quang.pham@hust.edu.vn

like ABAQUS are gaining attention for their flexibility and capability to model multiphysics problems. ABAQUS can simulate phase transitions by embedding latent-heat effects into the enthalpy formulation of the heat-transfer equation, making it suitable for academic and industrial exploration of casting phenomena [14-18].

This study focuses on using ABAQUS to simulate the solidification of an aluminum alloy in a stepped mold design. The objective is to evaluate the effect of varying mold thickness on cooling rates, mushy-zone formation, and resulting microstructures. By mapping the transient thermal field and solidification fronts, this simulation serves as a practical tool for casting optimization and defect prediction.

METHODOLOGY AND MODELING

Modeling Phase Change (Melting/Solidification) in Abaqus

The governing heat transfer equation incorporating phase change using the enthalpy method is [17,18]:

$$\rho \frac{\partial H(T)}{\partial t} = \nabla \cdot (k(T)\nabla T) + Q \tag{1}$$

where ρ is the material density (kg/m^3), *H(T)* is the enthalpy as a function of temperature (J/kg), *k(T)* is thermal conductivity (W/m.k), T is the temperature (^{o}C or K) and Q is internal heat generation.

The enthalpy *H(T)* includes latent heat *(L)* through temperature-dependent specific heat capacity in the solidification range between solidus T_S and liquidus T_L. [17,18]

$$H(T) = \int_{T_L}^{T_S} C_p(T')dT' + L \cdot f(T) \tag{2}$$

Where $C_p(T)$ is specific heat capacity, L is latent heat of fusion and *f(T)* is melt fraction *(0 to 1)* during solidification.

Mold–Casting Model and Mesh (Steel Mold)

Figue 1 shown the mesh model illustrated below represents a stepped mold system comprising two material regions: the casting (aluminum alloy) and the surrounding mold. The stepped mold design aims to create variations in mold wall thickness across different areas, thereby inducing non-uniform cooling rates during heat transfer. The use of a 2D axisymmetric model [16] in thermal or casting simulations is entirely reasonable and optimal when the mold–casting system exhibits rotational symmetry. This means that if we 'cut' the geometry along a plane through the axis of symmetry, the remaining section can represent the entire object when rotated about that axis.

DCAX4 axisymmetric thermal elements were used. A refined mesh was applied near the mold-metal interface. Transient nonlinear heat conduction was solved using ABAQUS's implicit solver [16].

- Number of elements: 428
- Number of nodes: 464

- Time per step: 0.050 s
- Total simulation time: 2.50 s

Table – Thermal Properties of Casting Alloy and Steel Mold

Table 1: Thermal Properties of Casting Alloy and Steel Mold [19].

Physical Property	Aluminum Alloy (Solid)	Aluminum Alloy (Liquid)	Steel Mold
Temperature (°C)	577	638	110
Density (kg/m^3)	2700	2380	7800
Specific Heat (J/kg·K)	904	1205	460
Thermal Conductivity (W/m·K)	92	123	50
Latent Heat of Fusion (J/kg)		360,000	

Initial and Boundary Conditions

Initial Condition:

- Pouring temperature: 700 °C
- Mold: 110 °C

Boundary Conditions:

- Convective heat transfer to the environment: $q = h(T - T_{env})$
- Mold temperature: assumed as Dirichlet or Robin boundary condition.
- Convective heat transfer with ambient at 25 °C, heat transfer coefficient: 20 W/m²·K.

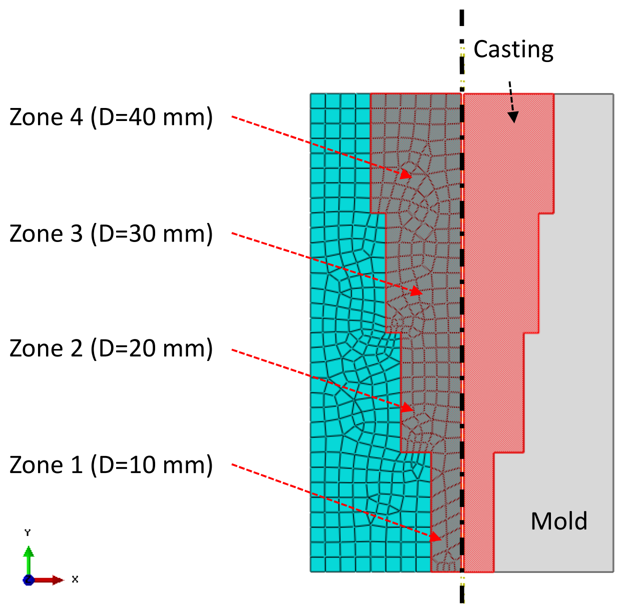

Figure 1: Stepped Mold – Casting Model and Mesh

RESULTS AND DISCUSSION

Temperature Evolution Results in ABAQUS Simulation

The cooling behavior captured at the center and near boundaries of the casting zones reveals a clear thermal lag in thicker regions. Center locations cool gradually, with temperatures

remaining high beyond 1.5 s in the thickest zones. This promotes coarse grain formation and can increase shrinkage-porosity susceptibility.
In contrast, boundary regions—especially in thin-walled sections—cool rapidly due to higher surface area-to-volume ratios. Temperatures near the mold interface can drop below 300 °C within 0.5 s, encouraging fine grains but raising the risk of surface cracking when thermal gradients are excessive.

Figure 2. presents the cooling curves at the center of four casting zones corresponding to the stepped mold design. The temperature at all centers begins around 700 °C and gradually decreases over time, indicating a slow cooling rate.

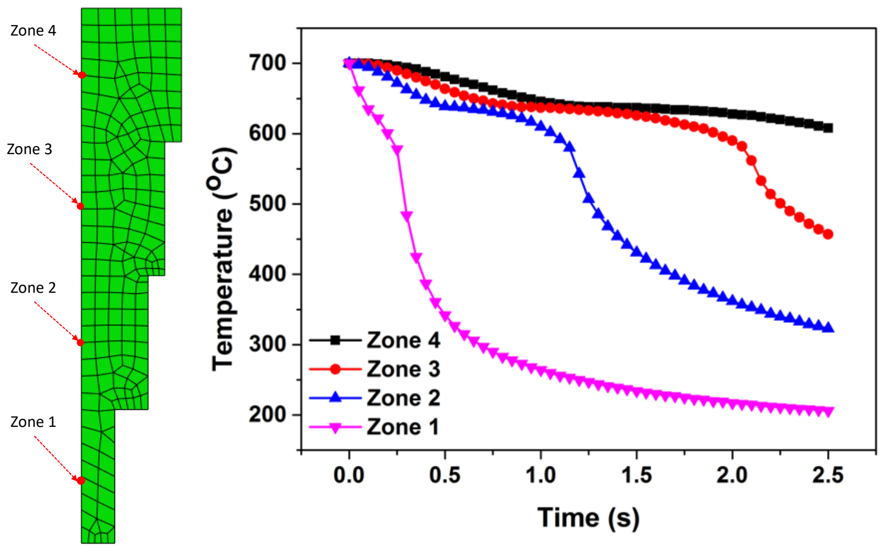

Figure 2: The cooling curves at the center of four casting zones

The curves exhibit gentle slopes, suggesting slow heat dissipation due to the central location being thermally insulated from the mold surfaces. The highest curve corresponds to the thickest casting region, which shows the slowest cooling rate, leading to delayed solidification and higher susceptibility to shrinkage porosity or gas defects. Lower curves correspond to thinner regions, where faster cooling promotes finer microstructures and fewer casting defects. A clear distinction in cooling behavior appears between 0.5 to 1 seconds, especially between the thickest and thinnest regions. The deeper and thicker the casting region, the slower the cooling rate, increasing the risk of volume shrinkage and solidification defects.

Figure 3 shows the cooling curves at the near boundaries of the same casting regions. Unlike the center, the boundary temperature drops rapidly right after pouring.

The initial temperature is also ~700 °C but drops rapidly (e.g., the brown curve falls below 300 °C within 0.5 seconds), indicating a very high cooling rate. Boundaries in thinner regions exhibit the fastest cooling, while thicker sections cool more slowly. Regions in direct contact with the mold (especially thin sections) solidify quickly, often almost immediately after pouring. The cooling rate at the boundary is significantly higher than at the center. In thin-walled regions, excessive cooling may lead to fine microstructure but can also cause thermal cracks near the surface if not controlled properly. The simulation clearly shows that thermal behavior varies significantly between regions of different thicknesses. The center cools slower, especially in thicker parts, while the boundary cools rapidly, especially in thinner sections. This results in non-uniform microstructures and thermal stresses that can negatively affect the mechanical performance of the final casting.

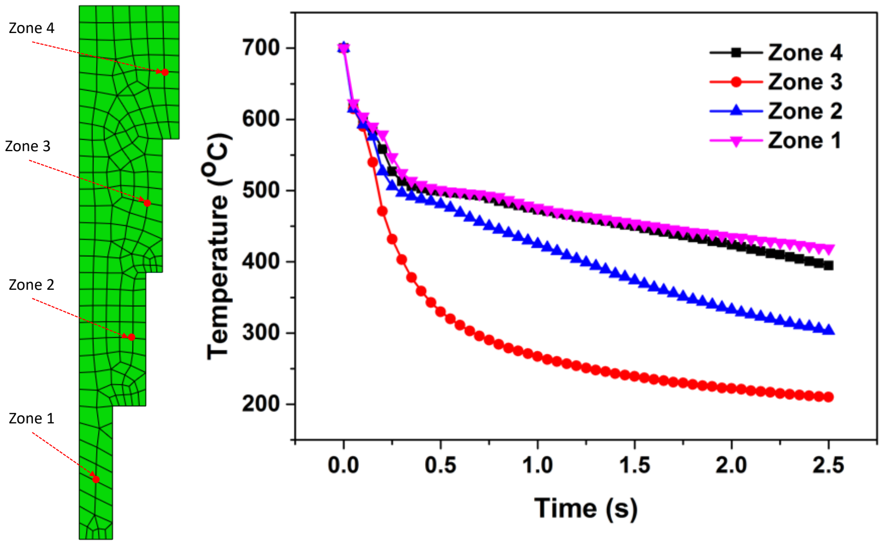

Figure 3: The cooling curves at the near boundaries of four casting zones

Semi-Solid Phase Development in the Casting

Figure 4 provides a clear chronological view of semi-solid region evolution. The simulation visualizes directional solidification initiated at mold interfaces, progressing inward. The stepped mold design intentionally creates thermal gradients, validating the choice of asymmetric mold geometry. Early solidification in thinner steps indicates that cooling occurs in layers, which aligns with directional solidification principles. However, thermal retention in thicker sections prolongs the mushy zone period, which can lead to macrosegregation if not properly managed [20].

This analysis focuses on the thermal behavior and phase transition of the alloy during the solidification process under the influence of non-uniform cooling rates caused by the stepped mold thickness.

Time = 0.00 s to 0.50 s: The entire casting remains in a molten state, predominantly red in color. No visible solidification occurs; heat has not yet dissipated significantly. Minimal temperature gradients appear, especially in thicker regions.

Time = 0.75 s to 1.00 s: Initial signs of solidification begin from the boundary areas near the mold surface, particularly in thinner regions. Semi-solid regions (light green/yellow) start to emerge. Heat dissipation occurs faster in thinner steps of the mold due to greater surface area exposure.

Time = 1.25 s to 1.50 s: Semi-solid zones expand further into the casting volume. Thermal gradients become more pronounced across different mold steps. Thinner sections solidify faster than thicker ones, confirming non-uniform cooling behavior.
Time = 1.75 s to 2.00 s: Most of the thin and intermediate regions are fully solidified. The thickest sections remain partially molten, especially at the center, shown by the persistence of red/orange colors. Clear asymmetry in cooling and solidification front progression.

Time = 2.25 s to 2.50 s: Nearly the entire casting has reached the solid or semi-solid phase. Residual molten pockets may persist in the thickest and most insulated regions, indicating a delayed solidification in those areas. The stepped mold geometry induces directional solidification, where thinner sections promote rapid heat extraction, leading to faster solidification.

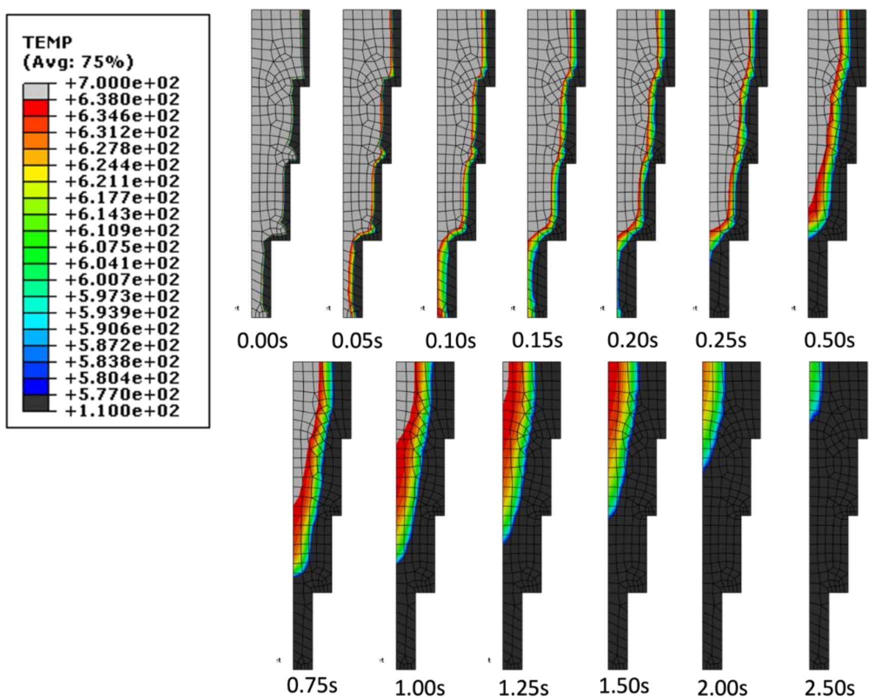

Figure 4: the evolution of the semi-solid region ranging from 0.00 seconds to 2.50 seconds

Conversely, thicker mold regions retain heat longer, causing delayed solidification and increasing the likelihood of shrinkage defects or porosity in those regions. The simulation demonstrates the formation of solidification fronts that move unevenly due to differences in wall thickness, validating the purpose of using a stepped mold in experimental design. This behavior also leads to microstructural variation throughout the casting: Fine dendritic or columnar grains in fast-cooled zones (outer layers), Coarse, equiaxed grains in the center of thick regions, Potential soft zones or segregation areas if cooling is uncontrolled.

Consistent with solidification theory, the simulation supports a zone-based microstructure expectation: *(i)* fast-cooling zones exhibit fine dendritic/equiaxed grains (typical hardness ~160–170 HB), *(ii)* moderate-cooling zones show columnar or mixed grains (~145–155 HB), and *(iii)* slow-cooling zones develop coarse grains with higher porosity risk (~130–140 HB) [1,2].

CONCLUSION

This study demonstrates that ABAQUS can effectively simulate aluminum alloy solidification by incorporating latent heat and solving transient heat transfer using a 2D axisymmetric model. The stepped mold design enabled the creation of non-uniform thermal gradients, allowing the study of differential cooling behaviors and their effects on solidification.

Key findings include:

- Slower cooling in thick regions results in coarse microstructures and higher defect risk.
- Rapid solidification in thin zones promotes fine grain structure but risks thermal cracking.
- Thermal simulations are crucial for optimizing mold geometry to balance structural integrity and casting performance.

The results validate ABAQUS as a powerful tool in early casting design and microstructural prediction. Future work can include coupling thermal analysis with mechanical stress simulations to further explore residual stresses and dimensional accuracy.

References

[1] Flemings M. C., *Solidification Processing*, McGraw-Hill, 1974.

[2] Campbell J., *Castings*, 2nd ed., Butterworth-Heinemann, 2003.

[3] Luo A. A., *Recent advances in aluminum alloy casting technology*, JOM, vol. 54, no. 11, pp. 42–48, 2002.

[4] Kou S., *Welding Metallurgy*, 2nd ed., Wiley, 2003.

[5] Duc. D. M., Hai. N. H., and Quang. P., *Simulation and experimental study on the steady conduction solution for continuous rheo-casting for A356 alloy*, Korean J. Met. Mater., Vol. 55, No. 3 (2017), pp. 202~208.

[6] Nguyen Hong Hai, Pham Quang., *Effect of Pressure on Solidification Process and Mechanical Properties During Semi-Solid Casting by Computational Fluid Dynamics (CFD)*. Advances in Materials. Vol. 7, No. 2, 2018, pp. 44-49.

[7] Górny, M., Tyrała, E., *Effect of Cooling Rate on Microstructure and Mechanical Properties of Thin-Walled Ductile Iron Castings*. J. of Materi Eng and Perform, Vol. 22, 2013, pp. 300–305.

[8] Tang H. P. et al., *Effect of cooling rate on microstructure and mechanical properties of an Al-5.0Mg-3.0Zn-1.0Cu cast alloy*, Journal of Alloys and Compounds, Vol. 801, 2019, pp. 596-608.

[9] Juan Wang et al., *Effect of cooling rate on the microstructure and thermal expansion properties of Al–Mn–Fe alloy*, Reviews on Advanced Materials Science Vol. 61, 2022, pp. 265–275.

[10] Zare, M.A., Taghiabadi, R. & Ghoncheh, M.H., *Effect of Cooling Rate on Microstructure and Mechanical Properties of AA5056 Al-Mg Alloy*. Inter Metalcast, Vol. 16, 2022, pp. 1533–1543.

[11] Tai N. T., Duc D. M., Hai N. H., and Quang P., *Optimization of flow behavior in high-pressure die casting by the Pro/Engineer virtual manufacturing*, J. of Science and Technology 5A (201) (2013).

[12] Tai N. T., Duc D. M., Hai N. H., and Quang P., *Effect of pressure on microstructure and mechanical properties of A356 aluminium alloy during rheo-diecasting process (RDC),* J. of Science and Technology 5A (194) (2013).

[13] Pham Quang, *Numerical modeling and simulation of mold filling and solidification process of BS100 Grade A6 alloy in sand casting of excavator bucket coupling parts* , SCIREA Journal of Materials. Volume 10, Issue 1, February 2025, pp. 25-35.

[14] Duc D. M., Hai N. H., and Quang P., *Modeling of continuous rheo-casting the A356 alloy by finite element method (FEM),* Sci. Tech. Metals 46, 37 (2013).

[15] Nguyen H., Hoang D. Le, Q., and Quang P., *Numerical simulation and experimental study on effect of cooling rate on microstructure and strength of nanostructured materials*, Vietnam J. Sci. Technol., vol. 61, no. 4, Jun. 2024.

[16] Abaqus/CAE User's Guide: Abaqus 6.14, © Dassault Systèmes, 2011.

[17] Abaqus/Theory Manual: *Uncoupled heat transfer analysis*, © Dassault Systèmes, 2011.

[18] Cengel Y. and Ghajar A., Heat and Mass Transfer: *Fundamentals and Applications*, 5th ed., McGraw-Hill, 2015.

[19] Brandes E. A., *Smithells Metals Reference Book (Seventh Edition),* Published by Butterworth & Co. Ltd (1983).

[20] Poirier D. R. and Geiger G. H., *Transport Phenomena in Materials Processing*, Springer, 2016.